ABDOMINAL IMAGING
Iran J Radiol. 2020 October; 17(4):e99611. doi: 10.5812/iranjradiol.99611.
Published online 2020 October 25. **Research Article**

Application of Gemstone CT Spectroscopy in the Evaluation of Abnormal Enhancement of Lesion Margin After Radiofrequency Ablation of Hepatocellular Carcinoma

Yuchang Yan [1, 2], Tao Jiang [2], Zhenghan Yang [1], Zhenchang Wang [1], Erhu Jin [1, *] and Zhenyu Pan [2]

[1]Department of Radiology, Beijing Friendship Hospital, Capital Medical University, Beijing, China
[2]Department of Radiology, Beijing Chaoyang Hospital, Capital Medical University, Beijing, China

[*]*Corresponding author*: Department of Radiology, Beijing Friendship Hospital, Capital Medical University, 95 Yong-An Road, Xicheng District, Beijing, China. Tel: +86-1063139339, Email: erhujin@263.net

Received 2019 December 02; **Revised** 2020 September 30; **Accepted** 2020 October 11.

Abstract

Background: Accurately assessing the efficacy of radiofrequency ablation for hepatocellular carcinoma (HCC), and early detection of tumor residues or recurrence after radiofrequency ablation is important to improve the prognosis of patients with HCC.
Objectives: To investigate the application of gemstone spectral imaging in the evaluation of abnormal enhancement of the edge of HCC after radiofrequency ablation.
Patients and Methods: From November 2013 to April 2019, patients with HCC admitted to the department underwent regular gemstone spectral imaging and energy spectrum analysis after radiofrequency ablation. The abnormal enhancement within and around the radiofrequency ablation lesion was observed, and the energy spectrum data of the radiofrequency ablation lesion and the abnormal enhancement focus were measured.
Results: A total of 133 lesions with marginal enhancement following radiofrequency ablation were included. Of these lesions, 62 were eventually diagnosed as inflammatory reaction zone, and 71 were diagnosed as residual or recurrent HCC. The results of energy spectrum analysis showed that there was a statistically significant difference in the iodine concentration between the inflammatory reaction zone and the residual or recurrent HCC ($P < 0.001$). The iodine concentration in the inflammatory reaction zone was lower than the iodine concentration in the residual or recurrent HCC (9.70 ± 3.00 100 μg/mL vs. 13.24 ± 4.51 100 μg/mL). In the enhanced arterial and portal venous phases, the difference between the slope of the energy spectrum curve of the inflammatory reaction zone and the residual or recurrent HCC was statistically significant ($P < 0.001$).
Conclusion: Gemstone spectral imaging can effectively differentiate residual or recurrent HCC from the inflammatory reaction zone after radiofrequency ablation. It is conducive to early detection of residual or recurrent tumors, helps clinicians formulate the next treatment plan, and improves the prognosis of patients.

Keywords: Gemstone Spectral Imaging, Hepatocellular Carcinoma, Radiofrequency Ablation

1. Background

According to the European Association for the Study of the Liver, among the global cancer-related deaths, liver cancer is in second place (1). In primary liver cancer, hepatocellular carcinoma (HCC) accounts for about 75% to 85% of primary liver cancer (1, 2). Due to viral hepatitis, HCC is a major public health problem in the Asia-Pacific Region (3). Only 15% - 20% of HCC cases are suitable for surgical resection. Radiofrequency ablation (RFA) has been most frequently used worldwide in the treatment of HCC (4, 5). According to European and American guidelines, RFA is the first line treatment option for patients at the early stage not suitable for liver surgery or transplantation (6, 7). According to reports in the literature, the local recurrence rate of HCC after RFA is approximately 14.1% - 58.1%. If early detection and RFA are used, the complete ablation rate could be increased to 77% - 99.7% (8). Therefore, accurate assessment of the efficacy of RFA is important to improve the prognosis of patients with HCC.

Conventional computed tomography (CT) uses mixed energy. After X-ray passes through the human body, low-energy X-ray (i.e. soft X-ray) is filtered out, resulting in hardening artifacts of the beam, resulting in the drift

of the CT value. Gemstone spectral imaging (GSI) has a unique technique of energy spectrum scanning and post-processing, which can obtain the energy spectrum parameters of the lesion, rather than rely solely on CT value as an index to observe and evaluate the lesion. GSI has been widely used in the diagnosis and treatment evaluation of HCC. A study conducted by Yang et al. (9) has shown that dual-energy CT is more helpful than conventional CT in distinguishing small HCC with or without microvascular invasion. Another study performed by Laroia et al. (10) has shown that GSI can more accurately characterize the benign and malignant intrahepatic lesions that conventional CT cannot determine. Color-coded iodine CT using dual-energy CT technology can detect HCC around iodized oil uptake (11). Some researchers used dual-energy CT to measure the iodine intake in HCC to assess the treatment response after radioembolism (12). However, as far as we know, there is no research that used GSI to identify the inflammatory response zone and residual tumor after RFA of HCC.

2. Objectives

The present study aimed to investigate the application of GSI in the evaluation of abnormal enhancement of the edge of HCC after RFA.

3. Patients and Methods

3.1. Patient Population

Our study was performed in accordance with the principles of the Declaration of Helsinki and its appendices. This study was approved by the Ethics Committee, scientific research unit, Beijing, China (2015-Scientific Research-28), and written informed consent was obtained from all patients. We collected patients with HCC in the scientific research unit from November 2013 to April 2019. Inclusion criteria were as follows: The patient was diagnosed with HCC, the patient was conscious and able to cooperate with the doctor for CT examination, and the patient had normal respiratory function and could tolerate a breath hold for 5 - 10 seconds. Exclusion criteria were as follows: For HCC with a long diameter greater than 5 cm, it was difficult for RFA to completely destroy the tumor tissue, and it was necessary to elect a second operation, and patients were not included in the study after the first RFA. The patient's consciousness was unclear, and the CT examination could not be performed in accordance with the doctor's request. The patient had serious adverse reactions during RFA or had severe discomfort and could not tolerate continued treatment. If the patient had a history of iodine allergy, the enhanced CT scan was prohibited. After RFA of HCC lesions, patients were reviewed regularly for one month, and three months.

3.2. CT Technique

Scanning was done using GSI (Discovery CT 750 HD, GE Healthcare, Chicago, Il., USA). The scanning range was from the dome to the lower edge of the liver. The GSI energy spectrum scanning mode was used to divide the two-stage dynamic enhanced scanning, and the single-source instantaneous (0.5 ms) kVp (140 kVp and 80 kVp) switching technique was used to set the automatic milliamp. In the enhanced scanning, a double-tube high-pressure syringe was used to inject 70 - 90 mL of non-ionic contrast agent iopromide 300 (Bayer Schering Pharma AG, Leverkusen, Germany) into the cubital vein, the injection speed was 3 - 5 mL/s, after the injection of the drug, 30 s - 35 s (arterial phase), and 70 s - 80 s (portal venous phase). For the conventional image, the CT slice thickness and the CT slice spacing were both 5 mm. Then the single energy image (70 keV) and the mixed energy image were reconstructed, and the CT slice thickness and the CT slice spacing were both 0.625 mm.

3.3. Quantitative Assessment

The GSI scanning technique was used to acquire single-energy images and energy spectrum images in the arterial phase and the portal vein phase, and then the images were analyzed using GSI Viewer analysis software. The parameters required for measurement and calculation included: (1) Measure the iodine concentration in the inflammatory reaction zone, residual or recurrent HCC, RFA lesion, and hepatic parenchyma; (2) measure the difference in the iodine concentration in the arterial phase and the portal vein phase of residual or recurrent HCC, iodine concentration difference (ICD) = I arterial phase-I portal vein phase; (3) measure the slope of the spectral curve, slope = (HU50 kev-HU100 kev)/50 kev.

The region of interest (ROI) was selected as follows: (1) Residual or recurrent HCC: Combined with the patient's enhanced scan image, if the lesion volume was large ($d > 1.5$ cm), the solid area of the lesion was selected to place a ROI, the measured area in our study was about 25 mm^2, and avoided necrosis and bleeding of the lesion. If the lesion was small ($d < 1.5$ cm), the largest level of the solid portion of the lesion was chosen to place the ROI, the measured area in our study was about 10 mm^2; (2) inflammatory reaction zone: ROI was placed in a clinically diagnosed inflammatory reaction zone. The measured area in

our study was about 10 mm^2. If the inflammatory reaction zone was relatively narrow, the maximum allowable ROI was placed according to the width of the inflammatory reaction zone; (3) RFA lesions: The ROI was placed in the RFA lesion area. The measured area in our study was about 25 mm^2. When selecting the ROI, the vaporized part was not included; (4) Normal hepatic parenchyma: The ROI was placed away from the edge of the RFA lesion (greater than 2 cm) and where no abnormally enhanced hepatic parenchyma was found on the enhanced scan. The measured area in our study was about 25 mm^2. After RFA, even if the tissue around the tumor did not appear abnormally enhanced, because it was close to the RFA lesion, its tissue may have changed due to heat, but there would have been no visible change in iodine intake to the naked eye. In order to avoid measurement errors, the specific countermeasures were as follows: (1) To avoid artificial measurement errors caused by bias in the selection of the position of the ROI, all data of the same lesion needed to be measured 3 times, and the average value was calculated as the final result; (2) when selecting the ROI, the attempt was made to avoid large blood vessels and intrahepatic bile ducts, and avoid obvious artifacts on the image; (3) the slope of the energy spectrum curve was calculated using the energy spectrum curve data table output by the system to find the specific values at the time of HU50 kev and HU100 kev.

For diagnosis of residual or recurrent HCC and the inflammatory reaction zone, all original images were blindly and independently judged by three senior imaging diagnostic radiologists; then the diagnostic conclusions were synthesized. The diagnosis conclusion of this study adopted the principle of minority subordination to the majority. If there were obvious differences in the diagnosis conclusions, the three experts conducted a collective discussion. If the conclusions could not be unified after the discussion, the patient was removed.

In the 83 patients, a total of 102 HCC lesions meeting the inclusion criteria were found and RFA was performed. After follow-up observation, a total of 133 abnormally enhanced lesions at the edge of the RFA lesion were found. Diagnosis criteria for residual or recurrent HCC: (1) Part of the lesion was removed by laparoscopy (some patients underwent laparoscopic RFA, if eligible, the clinician would remove some of the lesion during surgery and send it for pathological examination); (2) biopsy was performed to take tissue and pathological diagnosis of HCC was carried out; (3) according to the "EASL Clinical Practice Guidelines: Management of HCC" (1) issued by the European Association for the Study of the Liver in 2018, make a diagnosis; if qualitative difficulties are encountered, follow up and observe regularly, and finally make a clear diagnosis. After comprehensive evaluation, 133 abnormally enhanced lesions at the edge of RFA lesions of HCC were detected, of which 71 (53.4%) were diagnosed as residual or recurrent HCC; 62 (46.6%) abnormally enhanced lesions were clinically diagnosed as inflammatory reaction zones.

3.4. Statistical Analysis

First, the one-sample Kolmogorov-Smirnov test was used to test the data for normality. Continuous quantitative variables (e.g. iodine concentration) were summarized as the mean $\pm$ standard deviation. Categorical variables (e.g. gender) were presented as counts (percentages). The differences in continuous variables such as iodine concentration and slope of the energy spectrum curve were assessed by one-way analysis of variance (ANOVA), and multiple comparisons between the groups were performed using the Dunnett T3 test. The area under the receiver operating characteristic curve (AUROC curve) was used to determine the performance of the iodine concentration and the slope of the energy spectrum curve in distinguishing between residual or recurrent HCC and the inflammatory reaction zone. The optimal cutoff values were identified from the highest Youden index. The iodine concentration in the arterial phase and the portal vein phase of the residual or recurrent HCC were compared by paired t test. Statistical analysis was performed with SPSS (version 16.0; SPSS Inc, Chicago, Il, USA). For all tests, $P < 0.05$ was considered statistically significant.

4. Results

4.1. Patient Characteristics

A total of 83 patients met the study criteria, including 63 males and 20 females. The male to female ratio was 3.1: 1. The patients were 20 to 84 years old, with an average age of 57.96 $\pm$ 11.26 years. Of the 83 patients, 71 were hepatitis B patients (85.5%), eight were alcoholic cirrhosis patients (9.6%), and four were hepatitis C patients (1.3%). The patients with hepatitis had all suffered from hepatitis for many years. At the time HCC was found, the average number of years of hepatitis was 25.21 $\pm$ 13.19; the median was 24 years. Of the 71 patients diagnosed with HCC, 58 (81.69%) had elevated alpha-fetoprotein levels (the normal range is 0 - 9 ng/mL). At the time HCC was found, the average alpha-fetoprotein level was 265.71 $\pm$ 115.52 ng/mL.

4.2. Comparison of Iodine Concentration in the Arterial Phase

There were significant differences in the iodine concentration in the hepatic parenchyma, RFA lesion, inflammatory reaction zone, and residual or recurrent HCC during the arterial phase of enhanced scanning (F = 190.41, P < 0.001). Multiple comparative analyses showed that there were significant differences in the iodine concentration between residual or recurrent HCC and the hepatic parenchyma, RFA lesion and inflammatory reaction zone. The iodine concentration in the residual or recurrent HCC was higher than that in the inflammatory reaction zone. The iodine concentration in the inflammatory reaction zone was higher than that in the hepatic parenchyma, and the iodine concentration in the hepatic parenchyma was higher than that in the RFA lesion (Table 1 and Figures 1 and 2).

Table 1. Iodine Concentration in Different Tissues of Arterial Phase and Portal Vein Phase (Unit: 100 μg/mL)[a, b]

Group	Number of cases (n)	Arterial phase	Portal vein phase
RFAL	83	2.55 ± 1.30	4.15 ± 1.77
HP	83	5.47 ± 2.40	19.34 ± 6.18
IRZ	62	9.70 ± 3.00	17.53 ± 5.75
RRHCC	71	13.24 ± 4.51	18.50 ± 5.93

Abbreviations: HCC, hepatocellular carcinoma; HP, hepatic parenchyma; IRZ, inflammatory reaction zone; RFAL, radiofrequency ablation lesion; RRHCC, residual or recurrent hepatocellular carcinoma.
[a]Values are expressed as mean ± SD.
[b]Post hoc comparison results: I, Arterial phase: RRHCC > IRZ > HP > RFAL; All P values < 0.001. II-portal vein phase: [RRHCC = IRZ = HP] > RFAL. P values: > 0.05 and < 0.001.

4.3. Comparison of Iodine Concentration in the Portal Vein Phase

There were significant differences in the iodine concentration in the hepatic parenchyma, RFA lesion, inflammatory reaction zone, and residual or recurrent HCC during enhanced scanning in the portal vein phase (F = 156.99, P < 0.001). The results of multiple comparative analyses showed statistically significant differences in iodine concentration between the RFA lesion, and the hepatic parenchyma, residual or recurrent HCC, and inflammatory reaction zone. However, there was no statistically significant difference in the iodine concentration between the hepatic parenchyma, residual or recurrent HCC, and inflammatory reaction zone (P > 0.05) (Table 1 and Figures 1 and 2).

4.4. Comparison of the Slope of Energy Spectrum Curve Between The Arterial Phase and the Portal Vein Phase

The slope of the energy spectrum curve of the hepatic parenchyma, RFA lesion, inflammatory reaction zone, and residual or recurrent HCC was significantly different between the arterial phase and the portal vein phase of the enhanced scanning (arterial phase F = 37.69, P < 0.001) (portal vein phase F = 172.79, P < 0.001). The slope of the energy spectrum curve of the residual or recurrent HCC, hepatic parenchyma, RFA lesion and inflammatory reaction zone were different. The slope of the energy spectrum curve of the RFA lesion was higher than that of the hepatic parenchyma, the slope of the energy spectrum curve of the hepatic parenchyma was higher than that of the residual or recurrent HCC, and the slope of the energy spectrum curve of the residual or recurrent HCC was higher than that of the inflammatory reaction zone (Table 2).

Table 2. Slope of Energy Spectrum Curve in Different Tissues of Arterial Phase and Portal Vein Phase

Group	Number of cases (n)	Arterial phase	Portal vein phase
RFAL	83	2.02 ± 0.97	2.47 ± 0.88
HP	83	1.65 ± 0.67	1.20 ± 0.30
IRZ	62	0.82 ± 0.28	0.72 ± 0.20
RRHCC	71	1.26 ± 0.63	0.99 ± 0.28

Abbreviations: HCC, hepatocellular carcinoma; HP, hepatic parenchyma; IRZ, inflammatory reaction zone; RFAL, radiofrequency ablation lesion; RRHCC, residual or recurrent hepatocellular carcinoma.
[a]Values are expressed as mean ± SD.
[b]Post hoc comparison results: I-Arterial phase: RFAL > HP > RRHCC > IRZ; All P values < 0.05. II-portal vein phase: RFAL > HP > RRHCC > IRZ; All P values < 0.001.

4.5. Comparison of Iodine Concentration in the Arterial Phase of Enhanced Scanning Between the Residual or Recurrent HCC and the Inflammatory Reaction Zone

The area under the receiver operating characteristic (ROC) curve was 0.74, P < 0.001, and the 95% confidence interval was 0.66 - 0.83. The results showed that there was a significant difference in the iodine concentration between the residual or recurrent HCC and the inflammatory reaction zone during the arterial phase. The iodine concentration of the residual or recurrent HCC was higher than that of the inflammatory reaction zone (Table 3 and Figure 3).

4.6. Comparison of the Slope of Energy Spectrum Curve in the Arterial Phase of Enhanced Scanning Between the Residual or Recurrent HCC and the Inflammatory Reaction Zone

The area under the ROC curve was 0.73, P < 0.001, the 95% confidence interval was 0.64 - 0.82. The results showed

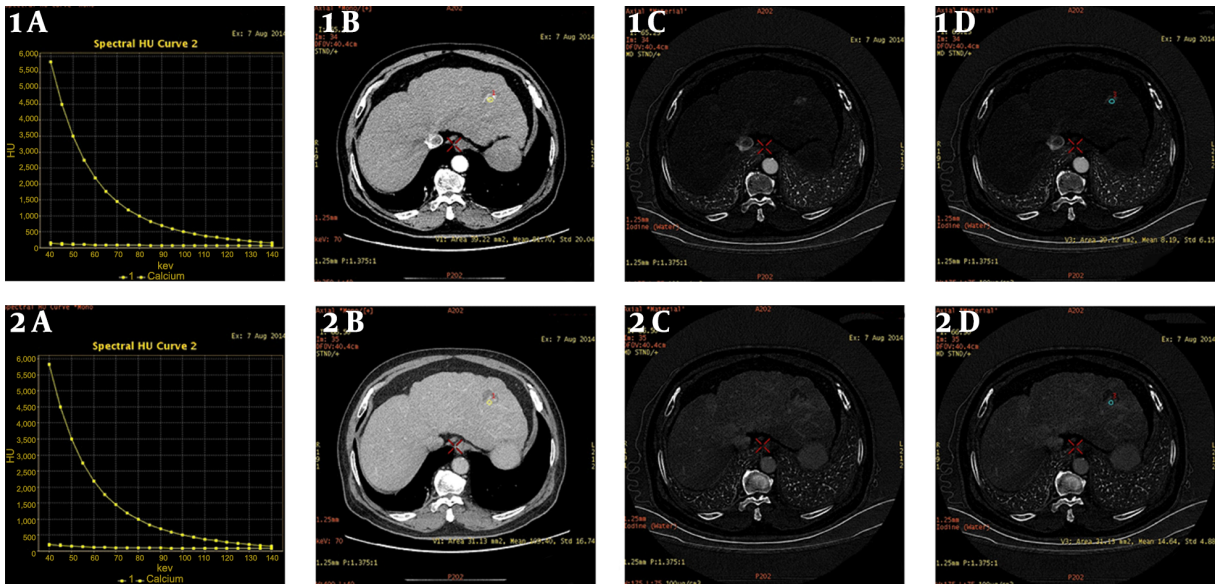

Figure 1. Male, 6 months after radiofrequency ablation of hepatocellular carcinoma (HCC). A, Arterial phase/portal phase spectrum curve of the recurrence of HCC, and the slope of the curve is basically the same; B, Arterial/portal phase of the enhanced lesion scan. The single-energy image of the pulse phase shows that the arterial phase lesions are significantly enhanced, and the portal vein phase lesions are basically of the same density; C and D, Arterial phase/portal phase iodine concentration map of the lesion enhancement scan, and the iodine concentration in the arterial phase was 8.19 (100 μg/mL), and the iodine concentration in the portal vein phase was 14.64 (100 μg/mL).

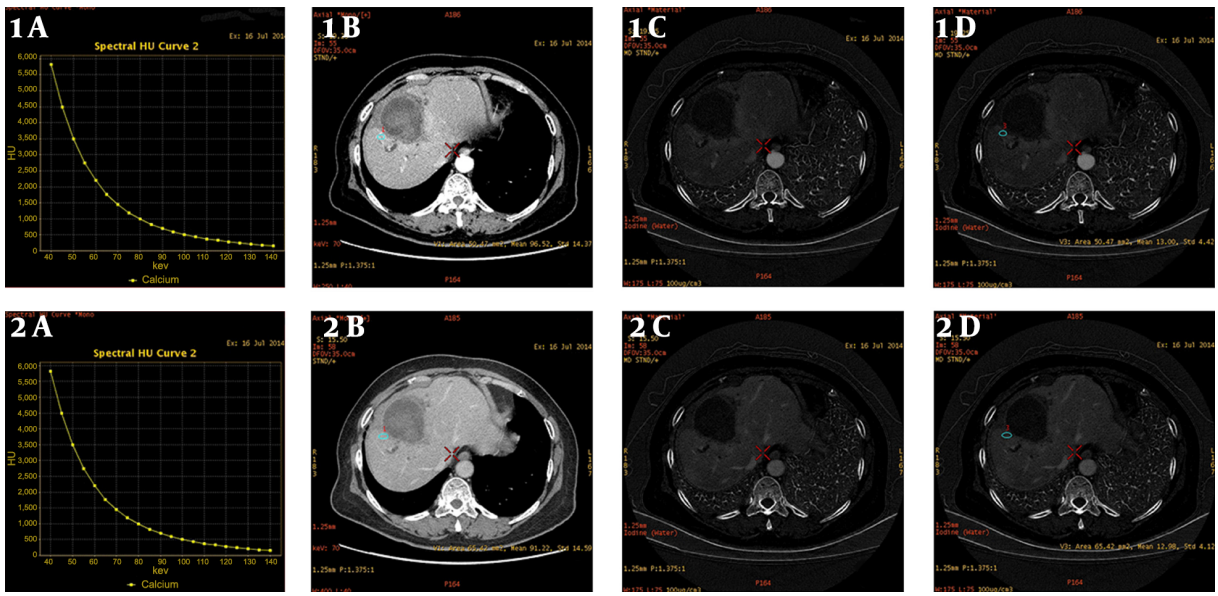

Figure 2. Male, 1 month after radiofrequency ablation of hepatocellular carcinoma (HCC). A, Arterial/portal phase of the energy spectrum curve of the inflammatory reaction zone, and the slope of the curve is basically the same; B, Arterial phase/portal phase of the lesion enhanced scan single energy image, the arterial phase is significantly enhanced, and the portal vein phase is basically the same density as the surrounding tissue; C and D, Iodine concentration maps of the arterial phase/portal phase of the enhanced lesion scan, and the iodine concentration of the arterial phase is 13 (100 μg/mL), and the portal phase iodine concentration was 12.38 (100 μg/mL).

that the difference in the slope of the energy spectrum curve between the residual or recurrent HCC and the inflammatory reaction zone in the arterial phase was statistically significant. The slope of the spectrum of the residual or recurrent HCC was higher than that of the inflammatory reaction zone (Table 3 and Figure 3).

Table 3. Results of ROC Curve Comparison of Energy Spectrum Data of RRHCC and IRZ: Diagnostic Indices of Selected Cutoff Points of ROC Analyses

Group	Cutoff value	Se (%) [95% CI]	Sp (%) [95% CI]	PPV (%) [95% CI]	NPV (%) [95%CI]
APIC (100 μg/mL)	13.440	57.7 [45.4 - 69.2]	90.3 [79.4 - 96.0]	87.2 [73.5 - 94.7]	65.1 [54.0 - 74.9]
SESCAP	1.135	56.3 [44.0 - 64.9]	85.5 [73.7 - 92.7]	81.6 [67.5 - 90.8]	63.1 [54.3 - 71.2]
SESCPVP	0.915	59.2 [46.8 - 70.5]	83.9 [71.9 - 91.6]	80.8 [67.0 - 89.9]	64.2 [52.7 - 74.3]

Abbreviations: APIC, arterial phase iodine concentration; CI, confidence interval; IRZ, inflammatory reaction zone; NPV, negative predictive value; PPV, positive predictive value; ROC, receiver operating characteristic; RRHCC, residual or recurrent hepatocellular carcinoma; Se, sensitivity; SESCAP, slope of the energy spectrum curve in arterial phase; SESCPVP, slope of energy spectrum curve in portal vein phase; Sp, specificity.

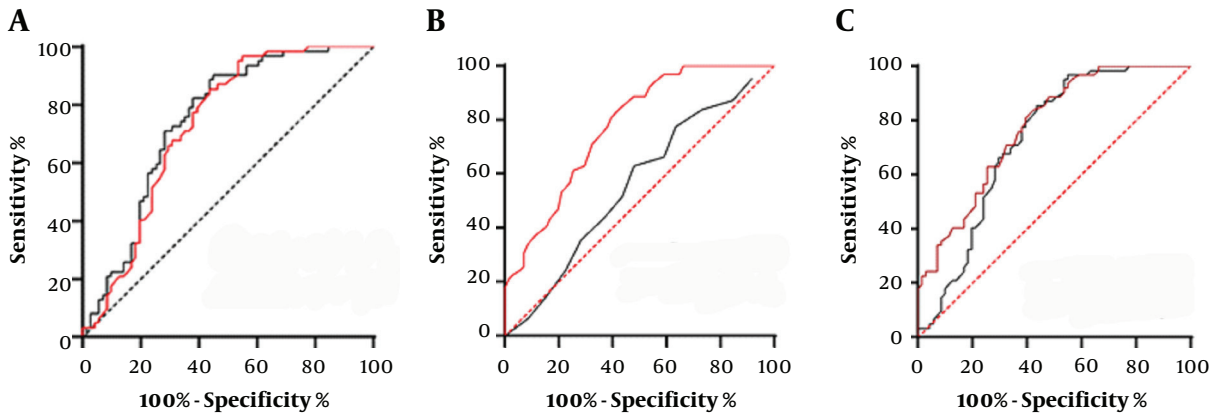

Figure 3. A, Receiver operating characteristic (ROC) curve comparison of iodine concentration and the energy spectrum curve of hepatocellular carcinoma (HCC) and the inflammatory reaction zone in the arterial phase (black line-iodine concentration, the area under the ROC curve was 0.74. red line-slope of the energy spectrum curve, the area under ROC curve was 0.73); B, ROC curve comparison of iodine concentration and energy spectrum curve of HCC and inflammatory reaction zone in portal vein phase (black line-iodine concentration, the area under ROC curve was 0.58. red line-slope of the energy spectrum curve, the area under ROC curve was 0.77); C, ROC curve comparison of the slopes of the energy spectrum curves between HCC and inflammatory reaction zone in arterial phase and portal vein phase (black line-arterial phase energy spectrum curve slope, the area under ROC curve was 0.73. red line-portal vein phase energy spectrum curve slope, the area under ROC curve was 0.77).

4.7. Comparison of Iodine Concentration Between the Residual or Recurrent HCC and the Inflammatory Reaction Zone in the Portal Vein Phase

The area under the ROC curve was 0.58, P = 0.25 > 0.05, and the 95% confidence interval was 0.46 to 0.66. The results srehowed that there was no significant difference in the iodine concentration between the residual or recurrent HCC and the inflammatory reaction zone in the portal vein phase scan (Table 3 and Figure 3).

4.8. Comparison of the Slope of Energy Spectrum Curve Between the Residual or Recurrent HCC and the Inflammatory Reaction Zone in the Portal Vein Phase Scan

The area under the ROC curve was 0.77, P < 0.001, and the 95% confidence interval was 0.70 to 0.85. The results showed that the difference between the slope of the spectrum curve of the residual or recurrent HCC and the inflammatory reaction zone during the portal vein phase was statistically significant (Table 3 and Figure 3).

5. Discussion

The inflammatory reaction zone (also called the benign reaction zone) is an abnormally enhanced area around the ablation zone, which is caused by heat-mediated inflammatory edema or granulation hyperplasia of the surrounding tissue (it is reported that the incidence is 89% at 1 month, 56% at 1 - 3 months, 22% at 6 months). The presence of a benign reaction zone affects the judgment of the efficacy, and the enhanced response carries enhanced information that may cover the residual lesion (13).

Studies have found that iodine concentration maps provide information on the distribution of venous contrast agents in end organs and may be useful in detecting high-vascular liver or kidney masses (14, 15). It has been reported by Lv et al. (16) and Yu et al. (17) that measuring iodine concentration with dual-energy CT may increase the accuracy when differentiating HCC from other hepatic neoplastic lesions. In this case, it was found that the enhanced arterial scanning phase could distinguish the

residual or recurrent HCC, inflammatory reaction zone, hepatic parenchyma, and RFA lesions through iodine concentration. The residual or recurrent HCC has the highest iodine concentration. ROC curve analysis of the residual or recurrent HCC and inflammatory reaction zone shows that the optimal cutoff value of iodine concentration is 13.44 (100 μg/mL). At this cutoff point, the sensitivity was 57.7%, [95% confidence interval (CI) = 45.4 - 69.2], while the specificity was 90.3% [95% CI = 79.4 - 96.0], which is relatively high.

Study has shown that the slopes as well as the characteristics of the dual energy CT energy spectrum curve of HCC, liver hemangiomas, metastases and cysts were significantly different (18). Quantitative dual energy CT energy spectrum curve analysis may be used to improve the sensitivity for differentiating liver tumors. In this case, it was found that during the enhanced scanning of the arterial phase and the portal vein phase, the difference in the slope of the energy spectrum curve of the residual or recurrent HCC, inflammatory reaction zone, hepatic parenchyma, and RFA lesions was statistically significant. The slope of the spectrum curve of the residual or recurrent HCC was higher than the slope of the spectrum curve of the inflammatory reaction zone in both arterial and portal vein phases. In the ROC curve analysis, the slope of the spectrum curve of the residual or recurrent HCC was compared with the slope of the spectrum curve of the inflammatory reaction zone. The optimal cutoff value of the arterial phase was 1.135. At this cutoff point, the sensitivity was 56.3% [95% CI = 44 - 64.9], while the specificity was 85.5% [95% CI = 73.7 - 92.7], which is moderate. The optimal cutoff value of the portal vein phase was 0.915. At this cutoff point, the sensitivity was 59.2% [95% CI = 46.8 - 70.5], while the specificity was 83.9% [95% CI = 71.9 - 91.6], which is moderate.

At present, judgment of the treatment effect of RFA is mainly based on imaging standards to observe whether the density of the lesion has significantly decreased. In addition, the effective range of radiofrequency needle heating is evaluated during the operation to ensure that the maximum diameter of the lesion shown by the preoperative imaging examination is included. At the same time, the RFA range is appropriately enlarged to deal with the micro-invasive lesions around the lesion. During RFA, we can perform GSI of HCC and use the slope of the energy spectrum curve to identify whether the ROI is necrotic tumor tissue or surviving tumor tissue. This needs further research to confirm its application value.

This study has a limitation. The slope of the energy spectrum curve is a standardized algorithm; it cannot fully describe the characteristics of the curve, so it may have a certain impact on the results of this study.

In conclusion, our findings showed that GSI not only retains the advantages of conventional CT scanning, but also adds a number of energy spectrum parameters and introduces energy resolution, which provides more reference indicators for the qualitative diagnosis of liver tumors. GSI can effectively differentiate HCC from inflammatory reaction zone after RFA. It is conducive to early detection of residual or recurrent tumors, helps clinicians to formulate the next treatment plan, and improves the prognosis of patients.

Acknowledgments

The authors thank AiMi Academic Services (www.aimieditor.com) for English language editing and review services.

Footnotes

Authors' Contributions: Study concept and design: EJ and ZP. Analysis and interpretation of data: YY and EJ. Drafting of the manuscript: YY. Critical revision of the manuscript for important intellectual content: ZY, ZW, and EJ. Statistical analysis: TJ.

Conflict of Interests: There is no conflict of interest in this article. All authors agree with the results of the study and agree to publish them in your journal.

Ethical Approval: This study was approved by the Ethics Committee, author's unit, Beijing, China (2015-Scientific Research-28), and written informed consent was obtained from all patients.

Funding/Support: There was no funding or support.

References

1. European Association for the Study of the Liver. Electronic address EEE. Corrigendum to "EASL Clinical Practice Guidelines: Management of hepatocellular carcinoma" [J Hepatol 69 (2018) 182-236]. *J Hepatol*. 2019;**70**(4):817. doi: 10.1016/j.jhep.2019.01.020. [PubMed: 30739718].
2. Deng GL, Zeng S, Shen H. Chemotherapy and target therapy for hepatocellular carcinoma: New advances and challenges. *World J Hepatol*. 2015;**7**(5):787–98. doi: 10.4254/wjh.v7.i5.787. [PubMed: 25914779]. [PubMed Central: PMC4404384].
3. Zhou C, Peng Y, Zhou K, Zhang L, Zhang X, Yu L, et al. Surgical resection plus radiofrequency ablation for the treatment of multifocal hepatocellular carcinoma. *Hepatobiliary Surg Nutr*. 2019;**8**(1):19–28. doi: 10.21037/hbsn.2018.11.19. [PubMed: 30881962]. [PubMed Central: PMC6383007].

4. Xu XL, Liu XD, Liang M, Luo BM. Radiofrequency Ablation versus Hepatic Resection for Small Hepatocellular Carcinoma: Systematic Review of Randomized Controlled Trials with Meta-Analysis and Trial Sequential Analysis. *Radiology*. 2018;**287**(2):461–72. doi: 10.1148/radiol.2017162756. [PubMed: 29135366].
5. Song J, Wang Y, Ma K, Zheng S, Bie P, Xia F, et al. Laparoscopic hepatectomy versus radiofrequency ablation for minimally invasive treatment of single, small hepatocellular carcinomas. *Surg Endoscopy*. 2016;**30**(10):4249–57.
6. Kim GA, Shim JH, Kim MJ, Kim SY, Won HJ, Shin YM, et al. Radiofrequency ablation as an alternative to hepatic resection for single small hepatocellular carcinomas. *Br J Surg*. 2016;**103**(1):126–35. doi: 10.1002/bjs.9960. [PubMed: 26572697].
7. European Association For The Study Of The L, European Organisation For R, Treatment Of C. EASL-EORTC clinical practice guidelines: management of hepatocellular carcinoma. *J Hepatol*. 2012;**56**(4):908–43. doi: 10.1016/j.jhep.2011.12.001. [PubMed: 22424438].
8. Mulier S, Ni Y, Jamart J, Ruers T, Marchal G, Michel L. Local recurrence after hepatic radiofrequency coagulation: multivariate meta-analysis and review of contributing factors. *Ann Surg*. 2005;**242**(2):158–71. doi: 10.1097/01.sla.0000171032.99149.fe. [PubMed: 16041205]. [PubMed Central: PMC1357720].
9. Yang CB, Zhang S, Jia YJ, Yu Y, Duan HF, Zhang XR, et al. Dual energy spectral CT imaging for the evaluation of small hepatocellular carcinoma microvascular invasion. *Eur J Radiol*. 2017;**95**:222–7. doi: 10.1016/j.ejrad.2017.08.022. [PubMed: 28987671].
10. Laroia ST, Bhadoria AS, Venigalla Y, Chibber GK, Bihari C, Rastogi A, et al. Role of dual energy spectral computed tomography in characterization of hepatocellular carcinoma: Initial experience from a tertiary liver care institute. *Eur J Radiol Open*. 2016;**3**:162–71. doi: 10.1016/j.ejro.2016.05.007. [PubMed: 27504474]. [PubMed Central: PMC4968142].
11. Lee JA, Jeong WK, Kim Y, Song SY, Kim J, Heo JN, et al. Dual-energy CT to detect recurrent HCC after TACE: initial experience of color-coded iodine CT imaging. *Eur J Radiol*. 2013;**82**(4):569–76. doi: 10.1016/j.ejrad.2012.11.014. [PubMed: 23238365].
12. Altenbernd J, Wetter A, Forsting M, Umutlu L. Treatment response after radioembolisation in patients with hepatocellular carcinoma-An evaluation with dual energy computed-tomography. *Eur J Radiol Open*. 2016;**3**:230–5. doi: 10.1016/j.ejro.2016.08.002. [PubMed: 27622200]. [PubMed Central: PMC5009187].
13. Tsuda M, Majima K, Yamada T, Saitou H, Ishibashi T, Takahashi S. Hepatocellular carcinoma after radiofrequency ablation therapy: dynamic CT evaluation of treatment. *Clin Imaging*. 2001;**25**(6):409–15. doi: 10.1016/s0899-7071(01)00333-3. [PubMed: 11733155].
14. Graser A, Johnson TR, Chandarana H, Macari M. Dual energy CT: preliminary observations and potential clinical applications in the abdomen. *Eur Radiol*. 2009;**19**(1):13–23. doi: 10.1007/s00330-008-1122-7. [PubMed: 18677487].
15. Kawaoka T, Aikata H, Murakami E, Nakahara T, Naeshiro N, Tanaka M, et al. Evaluation of the mRECIST and alpha-fetoprotein ratio for stratification of the prognosis of advanced-hepatocellular-carcinoma patients treated with sorafenib. *Oncology*. 2012;**83**(4):192–200. doi: 10.1159/000341347. [PubMed: 22890083].
16. Lv P, Lin XZ, Li J, Li W, Chen K. Differentiation of small hepatic hemangioma from small hepatocellular carcinoma: recently introduced spectral CT method. *Radiology*. 2011;**259**(3):720–9. doi: 10.1148/radiol.11101425. [PubMed: 21357524].
17. Yu Y, He N, Sun K, Lin X, Yan F, Chen K. Differentiating hepatocellular carcinoma from angiomyolipoma of the liver with CT spectral imaging: a preliminary study. *Clin Radiol*. 2013;**68**(9):e491–7. doi: 10.1016/j.crad.2013.03.027. [PubMed: 23702491].
18. Wang Q, Shi G, Qi X, Fan X, Wang L. Quantitative analysis of the dual-energy CT virtual spectral curve for focal liver lesions characterization. *Eur J Radiol*. 2014;**83**(10):1759–64. doi: 10.1016/j.ejrad.2014.07.009. [PubMed: 25088350].